A setup for transmission measurements of low energy multiply charged ions through free-standing few atomic layer films

V. Smejkal[a], E. Gruber[a], R.A. Wilhelm[b], L. Brandl[a], R. Heller[b], S. Facsko[b], F. Aumayr[a,*]

[a]*Institute of Applied Physics, TU Wien, Wiedner Hauptstr. 8-10/E134, 1040 Vienna, Austria, EU*
[b]*Helmholtz-Zentrum Dresden-Rossendorf, Institute of Ion Beam Physics and Materials Research, 01328 Dresden, Germany, EU*

Abstract

We report the design and testing of a setup for transmission measurements of multiply charged ions through free-standing films with a thickness of a few atomic layers. The investigation thereof can yield deeper insight into charge equilibration and pre-equilibrium stopping phenomena which can ultimately be used to specifically tailor and modify these materials.

Keywords: transmission measurements, highly charged ions, ion surface interaction, graphene, carbon nano membranes, ion charge loss, ion energy loss, equilibrium charge state

1. Introduction

Since the discovery of single layer graphene [1], 2D materials and films of just a few atomic layers have been in the spotlight of theoretical as well as of experimental research. Applications for these materials are manifold and range from miniaturised gas sensors [2–4] over chemical [5] to medical [6] applications. Due to their unique electronic properties, these materials are also of great interest for possible applications in future nanoelectronics [7].

One possibility to tailor 2D materials and thin films is by irradiation with ions in high charge states (HCI) [8–11]. For modelling of HCI induced damage, data on the energy deposition of the ions inside the target and the dissipation channels is indispensable [12].

Collision studies between ions and free-standing thin membranes are also of fundamental interest, because they bridge the gap between atomic collisions in gaseous and those in solid targets [13]. While most existing theories on heavy ion stopping at low velocities describe the stopping of a particle inside a solid by means of an equilibrium charge state [14–17], this concept loses its validity for targets with a thickness in the range of the equilibration length (in the order of a few nm [18, 19]) of the projectile [13].

By measuring the charge state distribution and energy loss of low energy multiply charged ions after transmission through free-standing foils, pre-equilibrium stopping values can be

*Corresponding author
Email address: aumayr@iap.tuwien.ac.at (F. Aumayr)

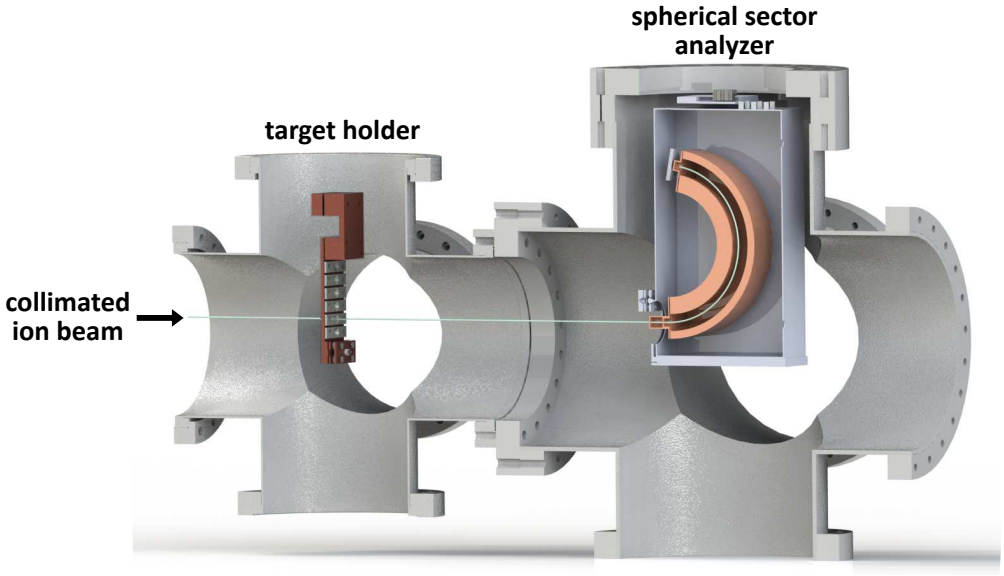

Figure 1: Cross section through the setup. The collimated ion beam (beam divergence below 0.5°) is guided onto a target holder that can hold multiple targets before it is charge state and energy selected by a 170° electrostatic spherical sector analyzer and detected with a microchannel plate detector.

accessed and valuable data for a deeper theoretical understanding of the underlying deexcitation processes can be gathered.

In this contribution we present an experimental setup designed for measuring charge state and energy distributions of low energy multiply charged ions transmitted through free-standing single or few atomic layer targets. First test measurements using Ar projectile ions and carbon nano membranes (CNMs) [20] as a target are presented.

2. Setup for transmission measurements

Multiply charged ions with energies in the order of 100 eV/amu are provided by the ECR ion source at the Institute of Applied Physics at TU Wien [21]. After extraction, the ions are mass-to-charge separated and collimated to a beam divergence below 0.5°. The beam is rectified using four sets of deflection plates before it enters the target chamber.

A cross section through the setup described in the following is shown in Figure 1. The targets that are used for transmission measurements are suspended on TEM grids. A target holder that can hold multiple of those grids is mounted on a 4-axes-manipulator. For beam diagnostics and beam alignment, a Faraday cup is positioned at the bottom of the target holder. Transmitted ions are charge state selected and energy analyzed using a 170° spherical sector electrostatic energy analyzer (comstock AC-903B) with an entrance and exit aperture of 1 mm in diameter. The mounting of the analyzer allows the detection of ions scattered into forward angles smaller than 3.9°. Particles are counted using a set of microchannel plates in the chevron configuration (comstock CP-602B) that is attached to the exit aperture of the analyzer.

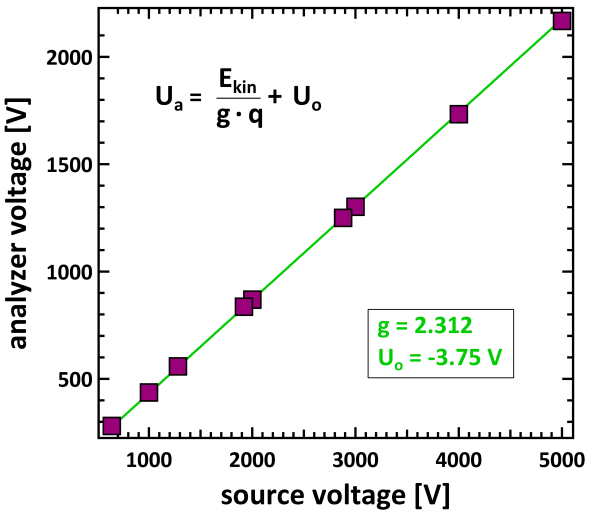

Figure 2: Calibration curve of the energy analyzer. The squares mark the measured data points while the solid line is the linear fit which defines the calibration parameters (c.f. text).

Calibration of the system

In order to obtain accurate energy loss data, we performed a calibration of the analyzing system. The pass voltage U_p for a particle with a given kinetic energy E_{kin} and charge state q through the spherical sector electrostatic energy analyzer is given by

$$U_p = \frac{E_{kin}}{q \cdot g} + U_o. \tag{1}$$

Here g is a geometry factor defined by the dimensions of the analyzer that can deviate from the one given by the manufacturer ($g_{man} = 2.283$) due to field inhomogeneities and imperfect geometry. U_o is an offset voltage accounting for a voltage difference between the read out voltage and the effective voltage between the analyzer's inner and outer electrode and a possible small tilt of the analyzer with respect to the beam direction.

For determination of the parameters g and U_o, primary peak positions without a target have been recorded at fixed ion source settings for a series of extraction voltages using Ar^{7+} and Ar^{9+} projectiles. By fitting the data points (squares in Figure 2) with Equation 1 (solid line in Figure 2), $g = 2.312$ and $U_o = -3.75$ were determined (for a discussion of possible errors see below).

3. Preliminary measurements and comparison to existing data

For the first measurements with the setup described above, CNMs suspended on a lacey carbon film on a copper TEM grid with a mesh width of 60 μm purchased from CNM Technologies, Bielefeld, Germany, have been used. They are created through cross-linking

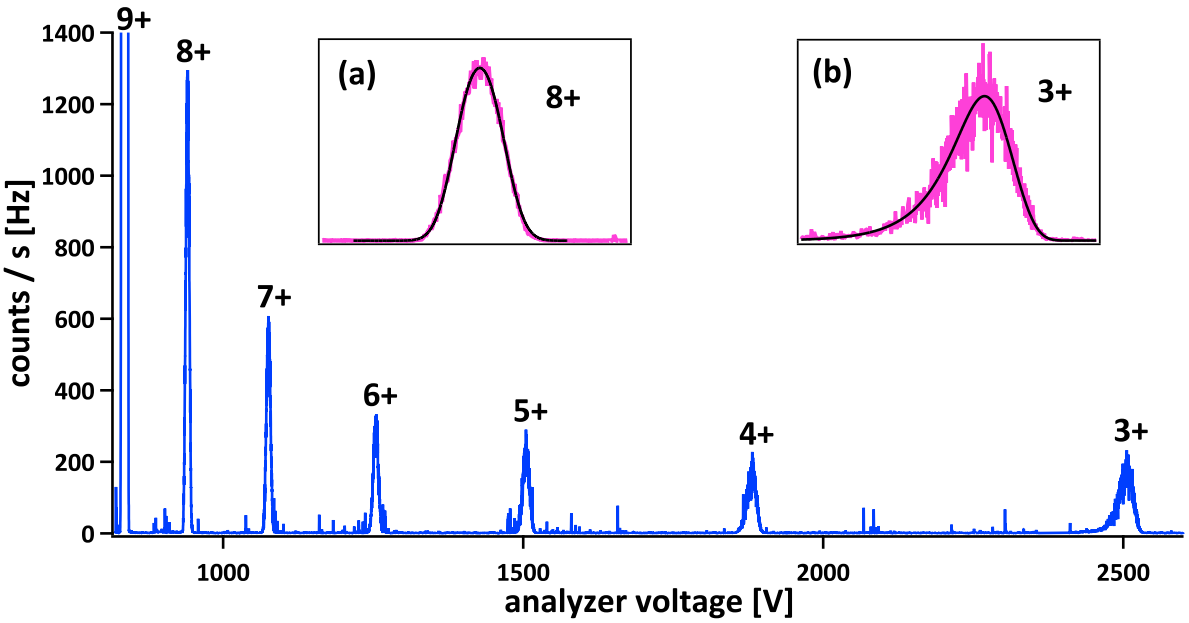

Figure 3: Transmission spectrum of Ar^{9+} ions at a kinetic energy of 17.3 keV through a carbon nano membrane. The primary Ar^{9+} peak is two orders of magnitude larger than the Ar^{8+} peak. The two insets show magnified peaks with the corresponding fit that is used for evaluation. For details see text.

by low energy electron irradiation of a self-assembled monolayer of aromatic molecules (1,1-biphenyl-4-thiol) grown on a Au substrate and have a thickness of 1 nm [22]. The pressure inside the experimental chamber was kept below $3 \cdot 10^{-9}$ mbar, such that charge exchange of the ion beam with residual gas atoms can be neglected.

Figure 3 shows a spectrum that was recorded with the setup for 0.43 keV/amu Ar^{9+} ions. The ions of different charge states are mapped to a series of distinct peaks by the electrostatic analyzer. Since a lower charge state corresponds to a higher pass voltage and the maximum pass voltage of the analyzer is 3500 V, the Ar^{2+} and the Ar^{1+} peak cannot be recorded at this projectile energy. The primary peak, which can be attributed to ions passing through damaged or ruptured parts of the foil, is about two orders of magnitude larger than the Ar^{8+} peak. The lacey carbon support has a thickness of at least 15 nm, which is enough for the ions to reach their equilibrium charge state according to Bohr's stripping criterion [23], which is approximately 0.3 for this energy regime. Thus the spectra taken are the result of the interaction of the ions with the CNM.

For the evaluation of the spectra, two things have to be taken into account:

(a) Looking at the low charge loss peaks, no straggling can be seen while the high charge loss peaks are very asymmetric. This requires two different energy distributions. While a Gaussian distribution is apt for the symmetric peaks, a Moyal distribution [24], which describes the energy loss of a particle traversing a thin foil, can be used to fit the peaks that exhibit straggling.

(b) The measured peaks are broadened by the spectrometer design. This can be included

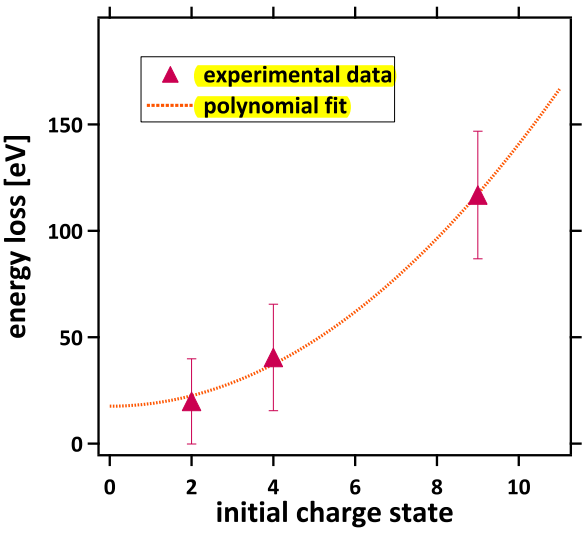

Figure 4: Energy loss of Ar^{q+} ions with a fixed kinetic energy of $E_{kin} = 5.8$ keV and an exit charge state of $q = 1$ plotted over the initial charge state q. A polynomial fit of second order (dotted) represents the data (triangles) very well.

by convolving the energy distribution with a function that is characteristic for the spectrometer. Details on the concept can be found in the supplemental material of [9].

The two insets in Figure 3 show the Ar^{8+} peak fitted with the convolution of a Gaussian distribution with the spectrometer function (left) and the Ar^{3+} peak fitted with the convolution of a Moyal distribution with the spectrometer function (right).

To compare our first results with existing data, spectra of ions with the same kinetic energy (i.e. 5.8 keV) and different initial charge states were evaluated. When plotting the energy loss of ions with an exit charge state of $q = 1$ over the initial charge state, the data points follow a polynomial fit of second order (see Figure 4). This behavior is the same as reported in [13] for the same target material (CNMs).

Accuracy estimation

The main contributions to the error of the energy loss measurements result from the fit to the data and the determination of the calibration parameters g and U_o. While the errors of the fit and g contribute to the statistical error, U_o can be split into a statistical contribution, which results in an uncertainty in the order of 10 eV, and a systematic contribution which will be discussed in the following.

The systematic error of U_o depends on the accuracy with which the initial energy of the ions can be determined, which is limited by an unknown positive plasma potential inherent to ECR ion sources. Two criteria are used to constrain the range for U_o: The upper limit is given by the estimate that the ions that have captured one electron on their passage through the CNM can at most show an energy gain which is given by the interaction with their image charge (see [25] for details). The lower limit of U_o is found by considering the limit of the

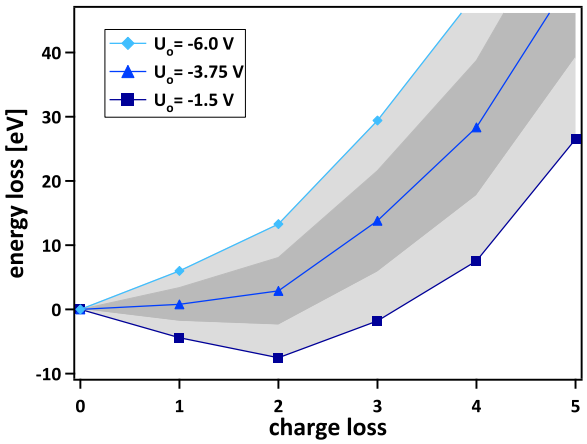

Figure 5: Range of systematic error of the measurements: The upper limiting curve (light blue dots) is given by the maximum shift of the extraction energies due to a positive plasma potential. The lower limiting curve (dark blue squares) is determined by a possible image charge interaction. The shaded area shows the error range. For preliminary evaluation, the center curve (medium blue triangles) corresponding to $U_o = -3.75$ V derived from the calibration curve in Figure 2 was used.

plasma potential inside the ECR ion source. For our type of source this limit lies around +25 V [27].

The shaded area in Figure 5 shows the validity range of U_o. Until further refinement of the calibration, a value of $U_o = -3.75$ V which is symmetric to the limits given above and consistent with the calibration in Figure 2 will be used. This induces a systematic error of the energy loss measurements of $\sigma^{sys}_{Eloss} = 2.25 * g * (q_{in} - q_{out})$ eV towards higher and lower energy losses (i.e. 5 eV (Ar^{8+}) - 31 eV (Ar^{3+}) for the energy loss measurements displayed in Figure 4).

4. Conclusion and outlook

We have designed and tested an experimental setup for energy loss and charge loss measurements of ions after transmission through free-standing films of a few atomic layers. The setup was calibrated and analyzed for possible sources of inaccuracies. After calibrating the setup, the evaluation of the first measured spectra reproduced a quadratic dependence of the energy loss on the incident charge state for projectiles with the same exit charge state.

The further scope of the experiment will comprise investigations on the transmission of medium charged ions through graphene and other 2D materials like MoS_2 or hexagonal BN. Spectra of CNMs will be taken at different analyzer angles to enter a regime of smaller projectile impact parameters and larger energy losses.

Acknowledgements

Partial financial support from the Austrian FWF (project no. I 1114-N20) is acknowledged.

References

[1] A. K. Geim, K. S. Novoselov, Nat. Mater. 6 (2007) 183–191.
[2] C. Stampfer, T. Helbling, D. Obergfell, B. Schöberle, M. Tripp, A. Jungen, S. Roth, V. Bright, C. Hierold, Nano Lett. 6 (2006) 233–237.
[3] A. B. Kaul, Nanotechnology 20 (2009) 155501.
[4] A. B. Kaul, H. M. Manohara, IEEE Trans. Nanotechnol. 8 (2009) 252–257.
[5] M. Chhowalla, H. S. Shin, G. Eda, L.-J. Li, K. P. Loh, H. Zhang, Nat. Chem. 5 (2013) 263–275.
[6] S. P. Adiga, C. Jin, L. A. Curtiss, N. A. Monteiro-Riviere, R. J. Narayan, WIREs Nanomed. Nanobiotechnol. 1 (2009) 568–581. doi:10.1002/wnan.50.
[7] A. Geim, I. Grigorieva, Nature 499 (2013) 419–425.
[8] R. Ritter, R. A. Wilhelm, M. Stöger-Pollach, R. Heller, A. Mücklich, U. Werner, H. Vieker, A. Beyer, S. Facsko, A. Gölzhäuser, F. Aumayr, Appl. Phys. Lett. 102 (2013) 063112.
[9] R. A. Wilhelm, E. Gruber, R. Ritter, R. Heller, A. Beyer, A. Turchanin, N. Klingner, R. Hübner, M. Stöger-Pollach, H. Vieker, G. Hlawacek, A. Gölzhäuser, S. Facsko, F. Aumayr, 2D Mater. 2 (2015) 035009. doi:10.1088/2053-1583/2/3/035009.
[10] J. Hopster, R. Kozubek, J. Krämer, V. Sokolovsky, M. Schleberger, Nucl. Instr. Meth. B 317 (2013) 165–169.
[11] J. Hopster, R. Kozubek, B. Ban-dEtat, S. Guillous, H. Lebius, M. Schleberger, 2D Mater. 1 (2014) 011011.
[12] D. Kost, S. Facsko, W. Möller, R. Hellhammer, N. Stolterfoht, Phys. Rev. Lett. 98 (2007) 225503.
[13] R. A. Wilhelm, E. Gruber, R. Ritter, R. Heller, S. Facsko, F. Aumayr, Phys. Rev. Lett. 112 (2014) 153201. doi:10.1103/PhysRevLett.112.153201.
[14] J. Ziegler, J. Biersack, U. Littmark, The stopping and ranges of ions in solids, New York: Pergamon Press (1985).
[15] H.-D. Betz, Rev. Mod. Phys. 44 (1972) 465.
[16] R. Herrmann, C. Cocke, J. Ullrich, S. Hagmann, M. Stoeckli, H. Schmidt-Boecking, Phys. Rev. A 50 (1994) 1435.
[17] M. Imai, M. Sataka, M. Matsuda, S. Okayasu, K. Kawatsura, K. Takahiro, K. Komaki, H. Shibata, K. Nishio, Nucl. Instr. Meth. B 354 (2015) 172–176.
[18] M. Hattass, T. Schenkel, A. Hamza, A. Barnes, M. Newman, J. McDonald, T. Niedermayr, G. Machicoane, D. Schneider, Phys. Rev. Lett. 82 (1999) 4795.
[19] T. Schenkel, A. Hamza, A. Barnes, D. Schneider, Prog. Surf. Sci. 61 (1999) 23–84.
[20] A. Turchanin, A. Gölzhäuser, Prog. Surf. Sci 87 (2012) 108–162.
[21] E. Galutschek, R. Trassl, E. Salzborn, F. Aumayr, H. Winter, J. Phys. Conf. Ser, 58 (2007), 395–398.
[22] A. Turchanin, A. Beyer, C. T. Nottbohm, X. Zhang, R. Stosch, A. Sologubenko, J. Mayer, P. Hinze, T. Weimann, A. Gölzhäuser, Adv. Mater. 21 (2009) 1233–1237.
[23] N. Bohr, Mat. Fys. Medd. Dan. Vid. Selsk 18 (1948).
[24] J. Moyal, , Philos. Mag. 46 (1955) 263–280. doi:10.1080/14786440308521076.
[25] J. Burgdörfer, P. Lerner, F. W. Meyer, Phys. Rev. A 44 (1991) 5674.
[26] Y. Miyajima, Y. Tison, C. Giusca, V. Stolojan, H. Watanabe, H. Habuchi, S. Henley, J. Shannon, S. Silva, Carbon 49 (2011) 5229–5238. doi:10.1016/j.carbon.2011.07.040.
[27] N. K. Bibinov, V. F. Bratesev, D. B. Kokh, V. I. Ochkur, K. Wiesemann, Plasma Sources Sci. Technol. 14 (2005) 109–128.